

Cocaine Self-Administration Alters Transcriptome-wide Responses in the Brain's Reward Circuitry

Supplemental Information

SUPPLEMENTAL TABLE LEGENDS

All supplemental tables are provided in Excel; See supplemental .zip file to download

Table S1: Differentially expressed genes (DEGs) calculated from pair-wise comparisons.

A complete list of DEGs (nominal p-value < 0.05; fold-change \pm 15%) in relation to saline controls (either S24 or SS) presented in Figure 1B. Each comparison is presented on a separate tab.

Table S2: Genes categorized by Patterns of expression.

A complete list of genes categorized as Pattern A, B, or C in each brain region. Log fold-change for all conditions when compared to the same baseline (S24) are included. Genes were categorized by their expression patterns and a fold-change cut off of \pm 15% was applied to each list to identify genes uniquely altered under each re-exposure condition. Each Pattern is presented on a separate tab.

Table S3: Overlap of genes categorized as Pattern A, B, or C across brain regions.

A complete list of genes categorized as Patterns A, B, or C that overlap across multiple brain regions. Fisher's exact tests revealed significant enrichment across lists. Comparisons reaching significance after multiple comparison correction (FDR) are bolded. Each pattern and direction of regulation is presented on a separate tab of the table.

Table S4: Overlap of genes associated with the addiction index (AI) across brain regions.

A complete list of genes associated with AI that overlap across multiple brain region. Fisher's exact tests revealed significant enrichment across lists. Comparisons reaching significance after multiple comparison correction (FDR) are bolded. Positive and negative associations are presented on separate tabs.

Table S5: Table of predicted upstream regulators of genes associated with AI.

A full list of predicted regulators of genes associated with AI and their activation z-scores. Activation z-Scores: positive = overrepresentation of targets activated by regulator; negative =

overrepresentation of targets repressed by regulator; no direction = no significant enrichment of activated or repressed targets; white = not a predicted upstream regulator.

Table S6: Overlap of genes categorized as Pattern A, B or C and associated with the AI within a brain region. A complete list of genes categorized as Pattern A, B, or C that overlap with those associated with AI within each brain region. Fisher's exact tests revealed significant enrichment across lists. Comparisons reaching significance after multiple comparison correction (FDR) are bolded. Comparison of Pattern/AI for each brain region are presented on a separate tab.

Table S7: Cell-type specific enrichment of genes categorized as Pattern A, B, or C or those associated with AI. Fisher's exact tests revealed significant enrichment of cell-type specific genes in those lists of genes categorized as Pattern A, B, or C or genes associated with AI within each brain region. Only comparisons reaching significance after multiple comparison correction (FDR) are presented.

Table S8: Transcriptome-wide associations with Factors 1 – 8. A complete list of the associations and p-values for each gene and Factor across all brain regions is presented. Each brain region is provided on a separate tab.

SUPPLEMENTAL FIGURES

A. Overview of qPCR Validation of RNAseq Setting Fold Change Cut-Off at 15% (Log₂(Fold Change = +/- 0.2)

Target	Assay ID	PFC	CPU	NAc
Sox18	Mm00956049_gH	Pattern A LFC = 0.563	Pattern A LFC = 0.629	Pattern A LFC = 0.567
Zfp763	Mm01349296_g1	Pattern A LFC = -0.189	Pattern A LFC = -0.190	Pattern A LFC = -0.194
Gam3	Mm01335316_m1	Pattern B LFC = -0.373	Pattern B LFC = -0.216	No Defined Pattern: CS LFC = -0.445
Etfb1	Mm00438866_m1	No Defined Pattern: CS LFC = -0.049	Pattern B LFC = 0.306	Pattern B LFC = 0.190
Map4b2	Mm01231699_m1	No Defined Pattern: CC LFC = 0.023	Pattern C LFC = -0.217	Pattern C LFC = -0.296
Loxk3	Mm01194047_m1	No Defined Pattern: CC LFC = -0.131	Pattern C LFC = -0.316	Pattern C LFC = -0.336
Six7	Mm01249607_m1	No Defined Pattern: CC LFC = -0.079	Pattern C LFC = -0.205	Pattern C LFC = -0.210
Creb1	Mm0091607_m1	No Defined Pattern: CS LFC = 0.253	Pattern C LFC = 0.178	Pattern C LFC = 0.265

Aput1	Mm03024075_m1	Internal Ctrl	Internal Ctrl	Internal Ctrl
Actb	Mm02519580_g1	Internal Ctrl	Internal Ctrl	Internal Ctrl

Fold Change of 15% and Validated by qPCR
 Fold Change <15% and Validated by qPCR

B. Representative Genes Showing Validation at 15% Fold Change

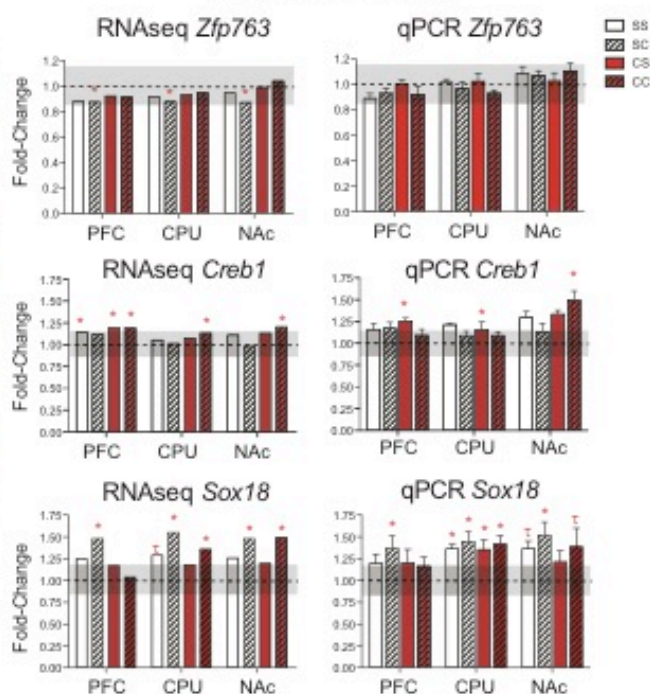
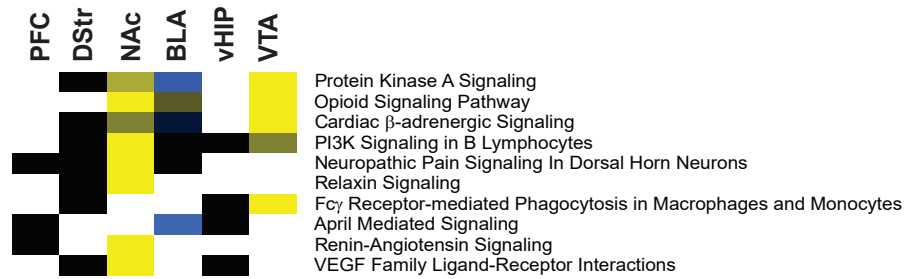
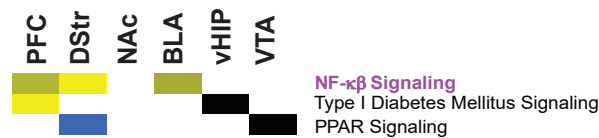


Figure S1: qPCR validation of Patterns in three brain regions reveals that fold changes of at least 15% are replicable. (A) List of 8 genes categorized as Patterns A, B, or C were validated using qPCR on technical replicates of the samples used in the RNA-seq experiment. Only those genes with a fold change of at least 15% were validated. (B-D) Expression of representative transcripts measured by RNA-seq and qPCR. Changes in expression of at least 15% in the RNA-seq data were validated by qPCR. This is exemplified by those changes in *Zfp763* (categorized as Pattern A but with <15% change in expression); *Sox18* and *Creb1* (Categorized as Pattern A or C, respectively with >15% change in expression). Gray shaded area on graphs indicates 15% change from S24. * = $p < 0.05$

A. Pattern A



B. Pattern B



C. Pattern C

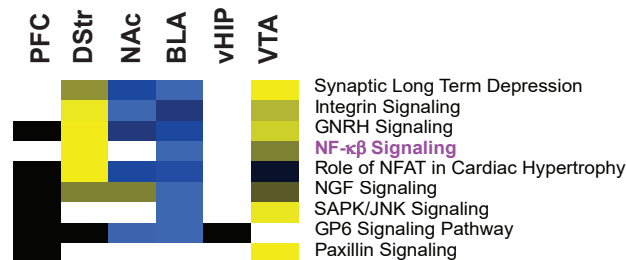
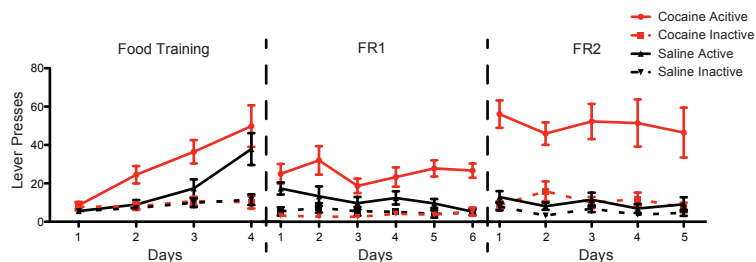


Figure S2: Similar pathways are associated with Patterns of gene expression across brain regions. (A) Pattern A was associated with protein kinase A signaling, while (B) Pattern B was dominated by NF κ B and PPAR, a nuclear receptor, signaling. (C) Pathways associated with Pattern C included synaptic long-term depression and NF κ B signaling. Pathways associated with both Patterns B and C are highlighted in purple. Only those pathways that met the following criteria were included: at least 1 brain region with an activation z-score >2 and p-value <0.01 . Activation z-Scores: positive (yellow) = overrepresentation of targets activated in pathway; negative (blue) = overrepresentation of targets repressed in pathway; no direction (black) = no significant enrichment of activated or repressed targets; white = not a predicted pathway.

A Behavioral Endpoints Represented in Factor Analysis



B Factor Loading for Behavioral Endpoints

	Factor 1	Factor 2	Factor 3	Factor 4	Factor 5	Factor 6	Factor 7	Factor 8
Total Intake	3.59	-0.40	-0.02	-0.03	-0.03	0.00	-0.01	-0.01
Avg Intake/day	1.87	-0.16	0.07	-0.06	0.03	0.07	-0.01	-0.09
Intake (Y/N)	0.49	-0.06	-0.01	-0.00	-0.01	-0.01	-0.01	0.01
Total Infusions	1.27	0.87	-0.01	0.09	-0.09	-0.03	0.15	0.05
Total Days SA	0.03	-0.14	-0.06	0.03	-0.02	-0.04	0.06	0.10
Total Lever Presses								
Active: Food	0.65	0.92	0.19	0.19	-0.57	0.13	-0.06	0.02
Active: FR1	1.06	0.85	-0.21	-0.21	0.05	-0.01	0.08	0.17
Active: FR2	1.67	0.97	0.34	0.60	0.22	0.01	0.06	-0.06
Inactive: Food	0.20	0.45	-0.20	0.37	-0.46	0.65	-0.02	0.06
Inactive: FR1	0.09	0.38	-1.23	0.33	-0.25	-0.27	0.30	-0.12
Inactive: FR2	0.61	0.62	-0.85	0.73	0.19	-0.25	-0.88	0.09
% Active Lever Presses								
Food	0.06	0.06	0.05	-0.03	-0.02	-0.07	0.00	0.00
FR1	0.09	0.06	0.10	-0.05	0.02	-0.01	-0.02	0.04
FR2	0.09	0.05	0.11	-0.02	-0.01	0.02	0.07	-0.01
Lever Presses/Day								
Active: Food	0.61	0.71	-0.05	0.21	-0.56	0.11	0.01	0.19
Active: FR1	0.89	0.97	-0.07	-0.26	0.10	0.07	-0.04	-0.06
Active: FR2	1.49	0.72	0.27	0.53	0.22	-0.02	0.10	0.01
Inactive: FR1	0.02	0.49	-0.83	0.22	-0.13	-0.16	0.16	-0.26
Inactive: FR2	0.48	0.40	-0.70	0.55	0.20	-0.23	-0.65	0.13
Grand Mean FR1	0.77	1.03	-0.15	-0.40	0.10	0.18	-0.08	0.03
Grand Mean FR2	1.50	0.75	0.27	0.54	0.24	-0.03	0.09	0.01
Consummatory Regulation	0.35	-0.33	0.24	0.72	0.07	-0.14	-0.05	0.04

Figure S3: Factor loading for behavioral endpoints used in factor analysis.

(A) Behavioral data represented in the factor analysis. All lever pressing data (food training, FR1, FR2; active vs. inactive) were included as variables in the factor analysis. Here we present a subset of the data aligned to the first day of each phase of self-administration. Because all animals had differing numbers of days in each phase, only those days in which the majority (>70%) of the animals in the study are presented. An image of the complete data set is presented in Figure 1D. (B) Factor analysis was used to reduce multidimensional behavioral endpoints to factors. The association of each factor with each behavioral endpoint included in the analysis is displayed.

Factors were positively (yellow), negatively (blue), or not associated (black) with each endpoint. These particular associations allowed for the interpretation of the how each factor related to various SA behaviors.

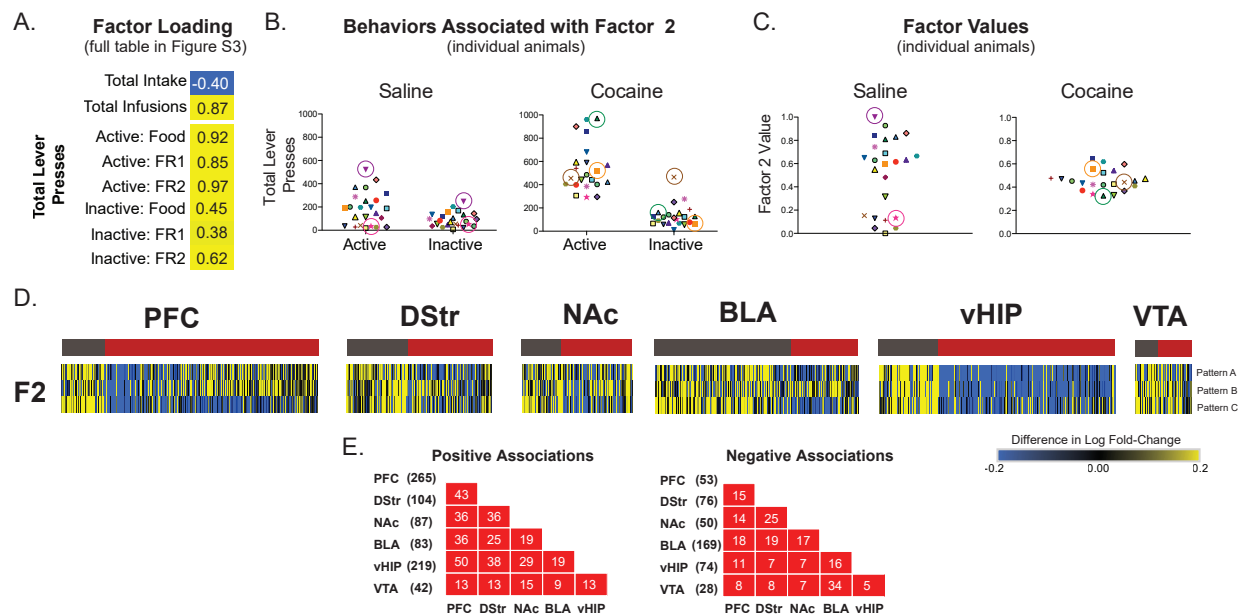


Figure S4: Factor 2 discriminates between baseline differences in saline animals. (A) Factor 2, in the factor analysis, was positively associated with both active and inactive lever pressing and negatively associated with intake. (B) Individual data for total number of lever presses in saline (left) and cocaine (right) for the entire SA experiment, including food training. (C) Individual factor values for Factor 2 for saline (left) or cocaine (right) animals. Animals with the greatest number of lever presses, but no intake, had highest factor value (\blacktriangledown in saline group). Animals with increased lever pressing coupled with high intake (\blacktriangle in cocaine group) had lower factor values. Finally, those animals with few lever presses and no intake (\star in saline group) had the lowest factor values. (D) Linear modeling was used to identify genes associated with Factor 2 within each brain region. Only genes with a $|\text{slope}| > 0.2$ and a nominal p-value of < 0.05 were investigated. (D) Genes were ranked by $-\log$ p-value signed by the slope of the association with Factor 2. Negative associations with Factor 2 are presented in gray and genes positively associated with Factor 2 are presented in red. (D) Heatmaps presented are transformed to indicate change in expression from SS controls. Blue = fold change in the negative direction from SS vs S24 and yellow = fold change in the positive direction from SS vs S24. These data indicate that changes in expression in transcripts associated with Factor 2 are most robust in the SS vs S24. This highlights the power of factor analysis to extract important information related to baseline behaviors and indicates that those differences are reflected in our transcriptomic data as well. (E) Overlap of genes positively (left) or negatively (right) associated with Factor 2 across brain regions, color-coded for significance. Total number of genes in each brain region listed in

parentheses and total number of genes overlapping between regions indicated in corresponding boxes. There is a high degree of overlap of transcripts associated with Factor 2 in all brain regions.

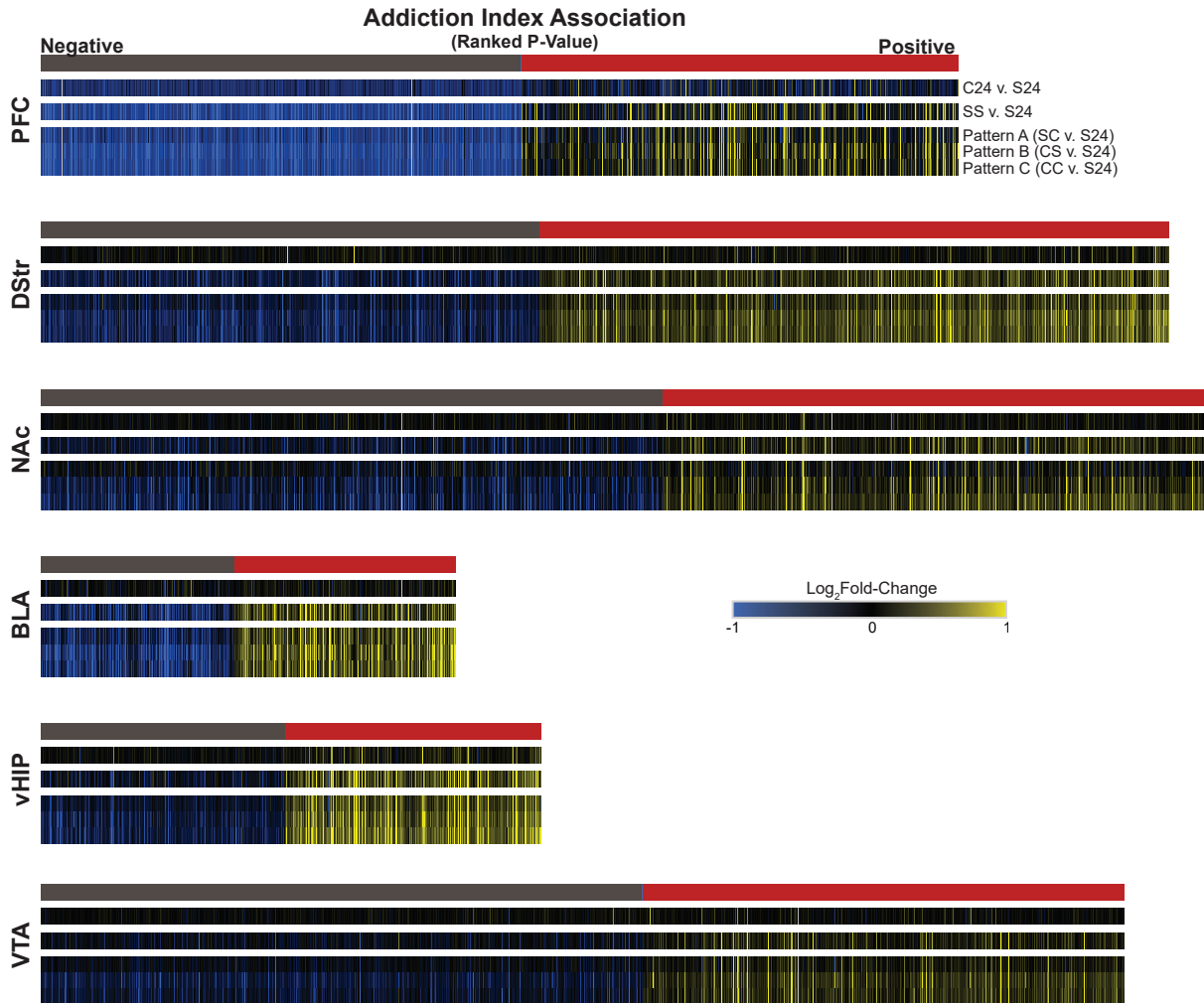


Figure S5: Raw heatmap of addiction index associated genes. (A-F) Raw expression of genes associated with AI in all brain regions for all groups when compared to the same baseline (S24). Log fold-change in expression of genes associated with AI and ranked by the sign of the association and $-\log(p\text{-value})$ (gray = negative associations; red = positive associations). In all groups but C24, genes that were negatively associated with AI (gray bar) were downregulated and genes positively associated with AI (red bar) were upregulated. In all brain regions, the strongest response was in comparisons representing either Pattern B or C, suggesting that that transcriptional response to re-exposure to context/cocaine is influenced by addiction-related behaviors during cocaine SA.

Addiction Index Pathways

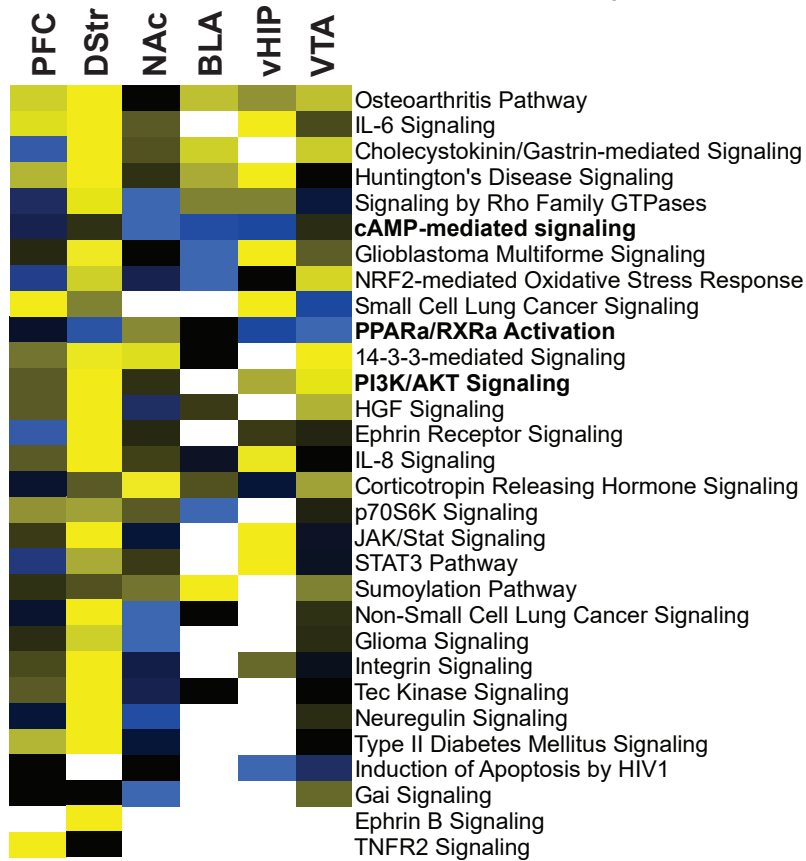


Figure S6: Pathways associated with the addiction index (AI). Ingenuity Pathway Analysis revealed genes associated with the AI, which were enriched for cAMP-mediated signaling, PPAR α /RXR α activation, and PI3K/AKT signaling among others. Activation z-Scores: positive (yellow) = overrepresentation of targets activated by regulator; negative (blue) = overrepresentation of targets repressed by regulator; no direction (black) = no significant enrichment of activated or repressed targets; white = not a predicted upstream regulator. Behavioral data analyzed using Kruskal-Wallis followed by Mann-Whitney Nonparametric Test; * $p < 0.05$; ** $p < 0.001$; data presented as mean \pm SEM.

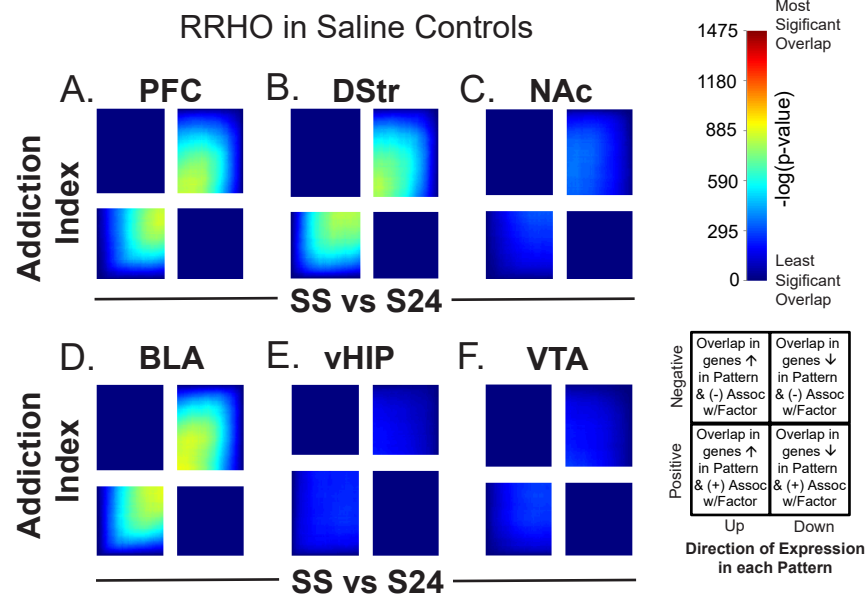


Figure S7: Overlap of transcriptional profiles related to the AI and saline controls. (A-F) RRHO plots reveal little overlap of genes positively or negatively associated with AI and up- or downregulated in saline control animals (SS vs S24). As predicted, little to no overlap of expression profiles was observed in NAc, vHIP and VTA. Overlap of expression was weak in PFC, DStr and BLA and similar to that observed in the comparisons with Pattern A. A key for these plots is provided.

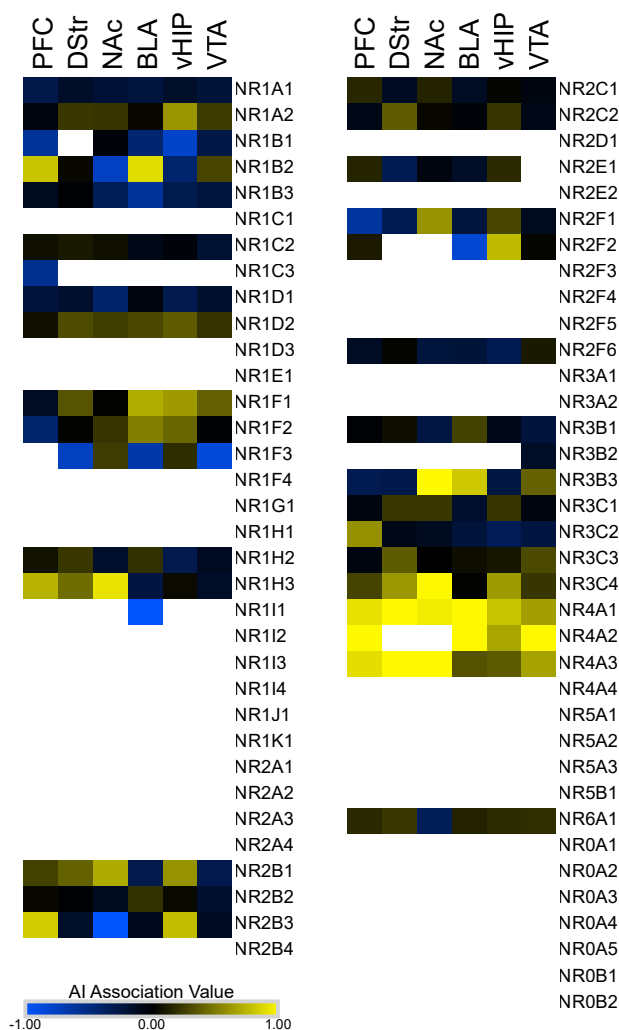


Figure S8: Full list of NR family members associated with the AI. Heatmap of association of all known nuclear receptors with the AI. Members of NR1 – 4 subfamilies are expressed throughout the reward circuitry. Strongest associations are found within NR2B and NR4A subfamilies. Yellow = positive association; Blue = negative association; Black = no significant association; white = expression not detected in our dataset.

SUPPLEMENTAL METHODS

Animals

In order to identify gene expression changes arising from environmental exposures, independent of genome sequence variation, genetically identical male C57BL/6J mice (6-8 wk-old) were used. Due to limitations of the study (e.g., number of operant boxes, number of animals, number of groups), we focused on males to limit the number of cohorts required. Male mice weighing 20-24 g were maintained on a 12 hr reverse light-dark cycle (lights on at 19:00) at 22-25°C with *ad libitum* access to food and water, except during training and testing when access to food was restricted. During self-administration testing mice were food restricted to 95% of their free-feeding weight. Mice were housed 5 per cage prior to jugular vein catheterization surgeries, at which point mice were housed individually. Following SA, those animals included in the withdrawal (WD) groups were rehoused with their original cage mates for the remainder of the experiment with *ad libitum* access to food and water.

Training, Surgery and Self-Administration

Food Training: Following 7-10 d of acclimation in the animal facility, mice were trained initially (3-10 d) for food reinforcement in standard operant chambers (Med Associates, St Albans, USA) equipped with 2 retracting levers (active and inactive), a cue light, and a house light. Animals were placed in operant chambers and illumination of the house light and extension of the levers signaled the beginning of the self-administration session. Active lever presses resulted in food reinforcer delivery followed by a 20 sec time-out period during which a cue light was illuminated and levers were retracted. Responding on the inactive lever was recorded, but resulted in no programmed consequence. Responding on the active lever was reinforced on a fixed-ratio one (FR1) schedule. Animals were considered to have acquired when they exhibited stable responding on the active lever (60% active/total lever presses) and >10 lever presses per 1 hr

session on an FR1 schedule of reinforcement. Once the animals met acquisition criteria, most were moved onto an FR5 schedule to further confirm acquisition of the task.

Cocaine Self-Administration: Following food training, mice were implanted with a jugular catheter (0.3 mm inner and 0.6mm outer diameter) under ketamine (100 mg/kg IP)-xylazine (10 mg/kg IP) anesthesia. Mice were administered MediGel® CPF containing carprofen (5 mg/kg) 1 d pre-op as an analgesic and intravenous ampicillin (0.5mg/kg) for infection prevention for 3 d post-op. In addition to standard chow, DietGel® Recovery (Westbrook ME) was provided to each mouse for 3 d post-op to aid in recovery. Mice were allowed to recover for 3-5 d before testing. Catheters were flushed daily with heparinized saline (10U/ml in 0.9% sterile saline) to ensure catheter patency. After recovery, mice began cocaine SA. For mice self-administering cocaine, active responses (FR1) resulted in a single (0.03ml) infusion of cocaine (0.5 mg/kg/infusion over 3.25 sec; cocaine HCL from the NIDA drug supply) and a discrete light cue was illuminated during the 20-s time-out period. Mice underwent 2 hr daily session for 10-15 d: 5-10 d on an FR1 schedule followed by 4-5 d of FR2 schedule. When animals self-administer drug on low effort schedules of reinforcement they defend a specific blood level of drug. Thus, in the case of changes in dose or FR requirement, animals will adjust responding to continue getting the same relative amount of drug (1) – referred to herein as “consummatory regulation.” In order to confirm that animals were in fact being reinforced by cocaine the FR requirement was increased. As predicted, animals assigned to cocaine SA (n=22), but not saline (n=24), pressed the active over inactive lever throughout the FR1 and FR2 phases (Figure 1D; corrected $p < 0.05$). Behavior is aligned to all animals’ first FR2 day in graphs, thus saline extinction is not easily observed.

The experiment was phased such that all six groups of mice were the same age at the time of euthanasia. Thus, animals were run in 2 cohorts. The first cohort was rehoused with their original cage mates and exposed to WD/forced abstinence for 30 d following their final trial. After 30 d of WD/forced abstinence, mice were given an IP injection of either cocaine (10 mg/kg) or

saline, placed back in their original operant chamber with house light illuminated; however, the levers were not extended. Animals were euthanized via cervical dislocation 1 hr after injection. All mice in cohort 1 were given saline injections (IP) for seven days prior to euthanasia to reduce stress in response to handling and injection. The second cohort was euthanized 24 hr after the final SA trial to assess the transcriptional alterations that occur following short-term WD (24 hr). Because all animals were socially isolated during food training and self-administration, cohort 2 was euthanized after prolonged social isolation. Small but significant differences in behavior were observed between the 2 cohorts, which most likely reflect slight differences in training paradigms (Figure 1A & D).

RNA Isolation, Library Preparation, and Sequencing

For all groups, brains were removed and sectioned on ice in a brain block (1 mm thick) and micropunches of six brain regions (PFC, NAc, DStr, vHIP, BLA, and VTA) were snap frozen on dry ice and stored at -80°C until use.

RNA was isolated as previously described (2) using RNeasy Mini Kit (Qiagen, Frederick, MD) using a modified protocol from the manufacturer allowing for the separation and purification of small RNAs from total RNA. Briefly, after cell lysis and extraction with QIAzol (Qiagen, Frederick, MD), small RNAs were collected in the flow-through and purified using the RNeasy MinElute spin columns and total RNA was purified using RNeasy Mini spin columns. Samples were treated with DNase to rid samples of genomic DNA and run on nanodrop and an Agilent Bioanalyzer 2100 to confirm RNA purity, integrity, and concentration. All samples' RIN>8.

Libraries were prepared using the TruSeq Stranded mRNA HT Sample Prep Kit protocol (Illumina, San Diego, CA). Briefly, poly A selection and fragmentation of 300 ng of RNA was converted to cDNA with random hexamers. Adapters were ligated and samples were size-selected with AMPur XP beads (Beckman Coulter, Brea, CA). Barcode bases (6 bp) were introduced at one end of the adaptors during PCR amplification steps. Library size and

concentration was assessed using Tape Station (Life Technologies, Grand Island, NY) before sequencing. Libraries were pooled for multiplexing (4 pools of ~60 samples with each group and brain region equally represented across each pool) and sequenced on a HighSeq2500 System using V4 chemistry with 50 base pair single-end reads at GeneWiz LLC (South Plainfield, NJ). Each pool was sequenced 8 times with the goal of obtaining ~25 million reads per sample. Initial quality control assessments revealed 43 samples, which did not meet standards for read depth and were excluded from analysis. Therefore, the final number of samples included in the analysis were between 5 – 8 per group apart from the CS group in VTA (N = 3).

qPCR Validation

Technical replicates were used to validate Patterns of expression across three brain regions. RNA (500 ng) from PFC, DStr, and NAc used for RNA-seq was converted to cDNA using High Capacity Reverse Transcriptase Kits (Catalog #: 4368814; ThermoFisher, Foster City, CA) according to manufacturer's protocol. qPCR was run for 8 genes of interest and 2 internal controls (Supplemental Figure S1) using Taqman® gene expression assays (Supplemental Figure 1A) and Taqman® Fast Universal Master Mix (Catalog #: 4444964; ThermoFisher, Foster City, CA) on an ABI Quant Studio Flex 7 according to the manufacturer's protocol. Six plates were run for each brain region using the following run parameters: 1 cycle (2 min @ 50°C followed by 2 min @ 95°C); 45 cycles (1 sec @ 95°C followed by 20 sec @ 60°C). Expression within each brain region was analyzed using the comparative Ct method (3). Each sample was normalized to its own internal controls (geometric mean of the Ct values for *Hprt1* and *Actb*) and calibrated to the average ΔCt for the S24 groups. In order to replicate the pair-wise differential expression analysis used for RNA-seq data, a Student's t-test was used to identify genes significantly different from S24.

Statistical and Bioinformatic Analyses

Behavior: Lever-pressing behavior and infusions were analyzed using a Kruskal-Wallis non-parametric test followed by Mann-Whitney Test to identify differences at individual time-points, treatments, or levers (cocaine vs saline; active vs inactive). Other behaviors were analyzed using ANOVA or Kruskal-Wallis tests depending on homozygosity of variance. All analyses were conducted using SPSS Statistical Software, V24 (IBM Analytics, Armonk, NY). To account for malfunctions in the operant chambers during SA sessions (e.g., broken tubing, stuck levers, etc.) we calculated the moving average of lever presses for the first 5 d of FR1 and the last 5 d of FR2 (averaged 3 d together each time). We then subtracted the grand mean of the FR1 moving average from the FR2 moving average as an indicator of consummatory regulation, which was included as a variable in the factor analysis.

Differential Expression Analysis: Sequencing short reads were aligned to the mouse mm10 genome using Tophat2 (4). QC analysis revealed a range of 18-60 million reads per sample with an average mapping rate of 90.2%. Read counts were generated using HtSeq-count against the Encode vM4 annotation. Stochastic outlier selection (5) was utilized to identify outliers prior to differential expression analysis. Samples with an outlier probability of >90% were excluded from analysis (4 samples out of 235 or 1.7%). Three of these belonged to one animal in which 4 of the 6 the brain regions investigated were predicted outliers; therefore, the entire animal was excluded from analysis. Data were filtered for low abundance transcripts by keeping only genes with more than 1 RPKM in at least 80% of samples per group. After filtering, pair-wise differential expression comparisons using Voom Limma were performed (6) and a nominal significance threshold of fold change >1.3 and $p < 0.05$ was applied.

Pattern Analysis: Each Pattern included genes that were differentially expressed from S24 ($p < 0.05$; fold change >15%) and also different from all other groups. For example, a gene that is

significantly increased in all groups compared to S24 and is further up-regulated by cocaine re-exposure is categorized as Pattern C. Importantly, even when genes are responsive to other stimuli, they are only categorized within Patterns A-C if the magnitude of change is greatest in that Pattern when compared to all other groups. Thus, we identified genes that are uniquely regulated by each stimulus in each brain region. Figure 2 highlights the fact that re-exposure to context alters expression of many genes in the same direction, but suggests that the magnitude of this changes is dependent on both a history of cocaine SA and re-exposure to context/cocaine.

Factor Analysis and Linear Modeling: Factor analysis was used to reduce the dimensions of the interdependent behavioral variables and help account for variability in the data due to differences in training, cohorts, and malfunctions in the operant chambers. All animals were included in the analysis. All behavioral measurements were first shifted to convert all data to non-negative values followed by $\log_2(x+1)$ transformation. For “total intake”, an additional variable referred to as “intake or not” was included to indicate whether total intake > 0. This accounted for the lack of cocaine intake in the saline groups. A standard factor analysis was performed using the scikit-learn package (7). A 10-fold cross-validation (CV) was utilized to choose the number of factors. We found that the CV log-likelihood was maximized with 8 factors. Therefore, the factor number was set to 8 when factor analysis was then applied to the whole dataset. The transformed data from the analysis was then used as a continuous variable for each factor. Differential analysis was conducted using Voom Limma to determine which factors were associated with gene expression (6).

Factor loading (Supplemental Figure S3) revealed three factors associated with the addicted-like phenotype. Factor 1 was positively associated with intake/infusions and was the Factor that most robustly discriminated between saline versus cocaine SA. Factor 3 was positively associated with active lever pressing and negatively associated with inactive lever pressing,

suggesting that Factor 3 is associated with an animal's ability to identify the reward-paired lever. Factor 4 was positively associated with active lever presses on FR2 and negatively associated with active lever presses on FR1. Factor 2 on the other hand, was positively associated with lever pressing (both inactive and active) and negatively associated with intake. We interpret this as reflecting baseline differences in behavior within our saline groups. Factors 5 – 8 were weakly associated with behaviors and were excluded from further investigation. A full list of transcripts and their associations with each factor are included in Supplemental Table S8.

Generation of an Addiction Index (AI): A composite score, or “addiction index,” of the three factors most strongly associated with an addictive phenotype was generated. This allowed us to identify animals with high performance scores across multiple behavioral endpoints associated with addiction and resulted in a continuous variable which could be used to identify genes that were positively or negatively associated with those behavioral endpoints. To calculate the index, factor values were linearly transformed to eliminate negative values. The transformation resulted in values that ranged from 0-1 for each factor: $[(\text{individual value} - \text{minimum value}) / (\text{maximum} - \text{minimum value})]$. The product of the transformed factors was calculated for each individual. Individual AI values as well as the transformed values for each factor are presented in Figure 4. As indicated, animals with high performance in all three factors have the highest AI but those animals with lower performance on any one factor have a reduced AI.

Enrichment Analysis: Fisher's exact tests were conducted using the Super Exact Test package in R as previously described (8).

Cell-type Enrichment Analysis: Enrichment for cell types were determined as previously described (9). Briefly, we used the Super Exact Test R Package (8) to evaluate statistical overlap between

our differential expression lists and genes expressed at least five times greater in one cell-type than in any other cell type in an established transcriptome study from cortical cells (10).

Rank Rank Hypergeometric Overlap (RRHO) Analysis: We applied an RRHO test to compare gene regulation between the comparisons representing each Pattern (e.g., Pattern A = differential expression between SC vs S24; Pattern B = differential expression between CS vs S24; etc.) and genes associated with the addiction index. RRHO identifies overlap between expression profiles in a threshold free manner to assess the degree and significance of overlap (11). Here we used a modified script that visualizes both positive and negative correlations and illustrates each quadrant separately based on the number of genes in each comparison as previously described (12). Full differential expression or association (Factors) lists were ranked by the $-\log(p\text{-value})$ multiplied by the sign of the fold change/slope of association. A one sided version of the test was used to look for over enrichment. RRHO difference maps were produced for each comparison by calculating for each pixel the normal approximation of difference in log odds ratio and standard error of overlap between the comparison representing the Pattern and the Factor. This z-score was then converted to a p-value and corrected for multiple comparisons across pixels (13).

Upstream Regulator and Pathway Analysis: Predicted upstream regulators and molecular pathways were identified using Ingenuity Pathway Analysis (IPA) Software (Qiagen, Frederick MD). These determinations were based on the log fold change of genes associated with each pattern ($p < 0.05$; fold change > 1.3) or factor ($p < 0.05$) analyzed. Upstream regulators and pathways were filtered by activation z-score (> 2) and p-value (< 0.001) as well as molecule (genes and proteins).

SUPPLEMENTAL REFERENCES

1. Norman AB, Tsibulsky VL (2006): The compulsion zone: a pharmacological theory of acquired cocaine self-administration. *Brain Res.* 1116:143-152.
2. Labonte B, Engmann O, Purushothaman I, Menard C, Wang J, Tan C, et al. (2017): Sex-specific transcriptional signatures in human depression. *Nat Med.* 23:1102-1111.
3. Schmittgen TD, Livak KJ (2008): Analyzing real-time PCR data by the comparative C(T) method. *Nat Protoc.* 3:1101-1108.
4. Trapnell C, Pachter L, Salzberg SL (2009): TopHat: discovering splice junctions with RNA-Seq. *Bioinformatics.* 25:1105-1111.
5. Jeroen Janssens FH, Eric Postma, Jaap van den Herik (2012): Stochastic Outlier Selection. *Tilburg Centre for Creative Computing.*
6. Law CW, Chen Y, Shi W, Smyth GK (2014): voom: Precision weights unlock linear model analysis tools for RNA-seq read counts. *Genome Biol.* 15:R29.
7. Pedregosa F, Varoquaux G, Gramfort A, Michel M, Thirion B, Grisel O, et al. (2011): Scikit-learn: Machine Learning in Python. *Journal of Machine Learning Research.* 12:2825-2830.
8. Wang M, Zhao Y, Zhang B (2015): Efficient Test and Visualization of Multi-Set Intersections. *Sci Rep.* 5:16923.
9. Bagot RC, Cates HM, Purushothaman I, Lorsch ZS, Walker DM, Wang J, et al. (2016): Circuit-wide Transcriptional Profiling Reveals Brain Region-Specific Gene Networks Regulating Depression Susceptibility. *Neuron.* 90:969-983.
10. Zhang Y, Chen K, Sloan SA, Bennett ML, Scholze AR, O'Keefe S, et al. (2014): An RNA-sequencing transcriptome and splicing database of glia, neurons, and vascular cells of the cerebral cortex. *J Neurosci.* 34:11929-11947.
11. Plaisier S.B. TR, Wong J.A., Graeber T.G. (2010): Rank-rank hypergeometric overlap: identification of statistically significant overlap between gene-expression signatures. *Nucleic Acids Res.* 38:169.
12. Seney ML, Huo Z, Cahill K, French L, Puralewski R, Zhang J, et al. Opposite molecular signatures of depression in men and women. *Biological Psychiatry.*
13. Benjamini Y, Drai D, Elmer G, Kafkafi N, Golani I (2001): Controlling the false discovery rate in behavior genetics research. *Behav Brain Res.* 125:279-284.